Eur. Phys. J. Plus (2020) 135:328
https://doi.org/10.1140/epjp/s13360-020-00328-5

THE EUROPEAN PHYSICAL JOURNAL PLUS

Regular Article

A coupled neutronic and thermal-hydraulic model for ALFRED

Mostafa Jamalipour[1], **Antonio Cammi**[2,a], **Stefano Lorenzi**[2]

[1] Department of Physics "G. Occhialini", University of Milano-Bicocca, piazza della Scienza 3, 20126 Milan, Italy
[2] Politecnico di Milano, Department of Energy, Nuclear Engineering Division – CeSNEF, via La Masa 34, 20156 Milan, Italy

Received: 21 May 2019 / Accepted: 11 March 2020 / Published online: 24 March 2020

Abstract A new method of Serpent–OpenFOAM coupling is developed as a multi-physics model for Advanced Lead Fast Reactor Demonstrator. The reactor core is simulated in Serpent, a continuous-energy Monte Carlo reactor physics code for neutronic analysis. A three-dimensional geometry is modeled for the calculation of neutronic parameters of the reactor initial core operation. The calculated parameters are evaluated with a good agreement compared to the available reference. The fuel assembly with the maximum power is pinpointed in order to be used for thermal-hydraulic analysis. A thermal-hydraulic model is developed to perform computational fluid dynamics calculation using OpenFOAM software, with an application of a heat conjugate transfer solver written in C++ language. A symmetric one-six of the fuel assembly with the highest power is considered in order to reduce the time of calculation. A multi-physics approach is adopted to map Serpent and OpenFOAM coupling for neutronic and thermal-hydraulic analysis. Moreover, a procedure is implemented in order to evaluate the convergence while coupling Serpent and OpenFOAM. With the implementation of multi-physics model, the maximum temperature of the fuel and coolant is investigated in order to observe any malfunctions. The results show that the coolant and the fuel temperature limits for the ALFRED's initial core are well preserved for the fuel assembly with the highest power.

List of symbols

c_p	Heat capacity ($\mathrm{J\,kg^{-1}\,K^{-1}}$)
D_k	Closure coefficient for $k-\varepsilon$ (–)
D_ε	Closure coefficient for $k-\varepsilon$ (–)
g	Gravity field ($\mathrm{m\,s^{-2}}$)
I	Identity tensor (–)
k	Turbulent kinetic energy ($\mathrm{m^2\ s^{-2}}$)
L_T	Turbulence length scale (m)
N_f	Number of fuel elements (–)
p	Pressure (Pa)

[a] e-mail: antonio.cammi@polimi.it (corresponding author)

P	Power (W)
P_{r}	Relative power variation (–)
P_{rel}	Relaxed power distribution (W)
s	Number of neutrons (–)
T	Temperature (K)
$\mathbf{u}$	Velocity field ($\mathrm{m\,s^{-1}}$)
U_0	Inlet velocity ($\mathrm{m\,s^{-1}}$)
α	Addition under relation factor (–)
K	Thermal conductivity ($\mathrm{w\,m^{-1}\,k^{-1}}$)
ε	Turbulent dissipation rate ($\mathrm{m^2\,s^{-3}}$)
μ_{T}	Turbulent dynamic viscosity (Pa s)
μ	Dynamic viscosity (Pa s)
ρ	Density ($\mathrm{kg\,m^{-3}}$)

1 Introduction

The European Lead Fast Reactor (ELFR) has been chosen as a candidate for the next generation of nuclear reactors. It is under research and development as a promising fast reactor to be applied in a closed-loop fuel cycle with the ability to reduce uranium consumption about two Orders of magnitude. ALFRED (Advanced Lead Fast Reactor Demonstrator) project aims to construct a $300\mathrm{MW_{th}}$ lead-cooled fast reactor demonstrator, connected to the electrical grid, predicted to start its operation in 2025 [1].

Applying liquid lead as a coolant in reactors introduces new advantages for plant simplifications and operation efficiencies compared to other sorts of coolant. However, the safety issues and design challenges also need to be taken into account. Furthermore, the large changes of coolant density with temperature are beneficial to promote natural circulation even in accidental conditions.

Its thermal cycle is identical to ELFR. While its coolant is considered liquid lead with the temperature between 673 and 753 K, its velocity is noted 1.4 m/s [2]. The core is composed of 171 wrapped hexagonal fuel assemblies. It consists of two inner and outer zones with MOX fuel. The inner zone contains 57 fuel assemblies with 21.7% of Pu while the outer one is designed with 117 fuel assemblies with the enrichment of 27.8%. Twelve control rods (CRs) are designed for reactor control during normal operation while four safety rods (SRs) are implemented for emergency shutdown. More information related to Gen-IV reactor design and its associated fuel cycle can be found in Refs. [3,4].

In this paper, ALFRED is modeled in Serpent a continuous-energy Monte Carlo reactor physics code for three-dimensional (3D) neutronic calculation of nuclear reactors. This code has already been applied for the neutronic calculation of Gen-IV reactors [5]. JEFF 3.1.1 is used for neutron cross section library. Other libraries have also been evaluated using serpent for neutronic calculations [6]. A 3D geometry is modeled for the reactor total core. Neutronic parameters such as control rod worth, neutron spectrum, power peaking factor, and the distributions of flux and power for the initial core are computed. Power distribution of fuel assemblies is obtained, and the fuel assembly with the highest power is specified. The neutronic parameters are evaluated with the calculated values provided in Ref. [2]. Based on the interface implemented in Serpent, the neutronic model of the fuel assembly with the highest power is modeled in order to obtain the power density distribution for each fuel pin. And it is inserted in thermal-hydraulic model for temperature calculation.

A multi-physics approach is carried out in order to observe the temperature and velocity distributions throughout the core using a thermal-hydraulic model for the fuel assembly with the maximum power during the first cycle. OpenFOAM software [7], a solver written in C++ language with the ability to perform computational fluid dynamics (CFD) analysis using finite volume discretization is applied. This code has already been evaluated for LFR thermal-hydraulic calculations [8,9]. The active part of the fuel assembly with one-six of symmetry is adopted for thermal-hydraulic analysis. The mass flow rate is inserted at the bottom of the model. The power density is inserted with the help of the interface implemented in Serpent. And the temperature distribution is calculated using a heat conjugate transfer (HCT) solver. Furthermore, the model of fluid flow is based on Reynolds-Averaged Navier–Stokes (RANS) equations for the conservation of mass, momentum and energy. In this paper, k-ε turbulent model is adopted to carry out CFD analysis for the compressible fluid flow. An approach is applied in order to couple neutronic and thermal-hydraulic models for the convergence in multi-physics calculations. Thermophysical properties of MOX fuel are obtained from Refs. [10–12] while the thermophysical properties for the fluid are taken from Refs. [13,14].

This paper consists of nine sections. Section 2 provides a brief description of ALFRED reactor with some details about fuel pin, fuel assembly, and control rods. Section 3 discusses the thermal-hydraulic model with thermophysical properties applied in the calculations, while Sect. 4 explains the model carried out for neutronic analysis. In Sect. 5, the power relaxation performed in the calculation as well as the method for the investigation of the convergence which is applied in multi-physics modeling is presented. Section 6 describes the methodology applied in coupling the neutronic and thermal-hydraulic models. In Sects. 7 and 8, the neutronic and thermal-hydraulic calculation results are obtained and discussed. Finally, a conclusion is drawn in Sect. 9.

2 ALFRED brief description

Advanced Lead-cooled Fast Reactor European Demonstrator (ALFRED) is a small-sized pool-type reactor with nominal operative power of 300 MW_{th}. It's a recently co-funded Lead-cooled European Advanced Demonstration Reactor (LEADER) project. The majority of reactor components such as the core, steam generators, and primary pumps are designed inside the reactor vessel. The reactor is placed in a lead pool. Its core consists of 171 fuel assemblies subdivided into two inner and outer parts with different plutonium enrichments; 21.7% is considered for 57 inner fuel assemblies while the outer part is designed with enriched fuel assembles of 27.8% with the number of 114. The core is surrounded by two rows of dummy elements as a reflector. In terms of cladding, Ti-15-15 steel was selected since it was previously validated for fast reactors (Phenix). The reactor is expected to have a five-year fuel residence time with five batches of cycle without reshuffling. Figure 1 shows its primary system and core layout. The specification of the reactor is shown in Table 1.

The fuel pin characteristics are adopted from ELFR [15] considering the maximum linear power rating (340 W/cm) and holding the assumption of 100 MWD/kg burnup peak for the ALFRED core. Also the central hole is implemented inside fuel pin for integrity of thermal-hydraulic performance. Annular U-Pu mixed oxide (MOX) is used as a fuel with two diverse enrichments of 21.7% and 27.8%. The oxygen-to-metal ratio for the fuel is 1.97 with theoretical density of 95%. Furthermore, 4.5% of ^{235}U enrichment is adopted for the fuel identical to typical pressurized water reactor (PWR). Figure 2 shows ALFRED fuel pin cross section, and Table 2 shows its specifications.

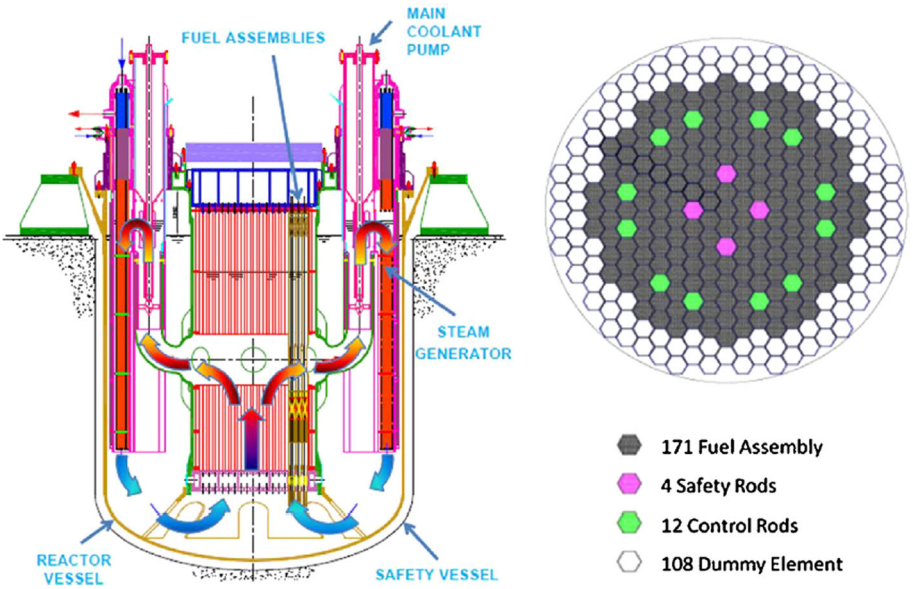

Fig. 1 ALFRED primary system and core layout

Table 1 ALFRED reactor specification

Parameter	Value
Thermal power (MW)	300
Maximum inner vessel radius (cm)	≈ 150
Fuel residency time (year)	5
Peak burnup (MWd/kg)	100
Maximum fission gas plenum pressure (MPa)	5
Clad material	Ti-15-15
Maximum fuel temperature (K)	2273
Maximum clad temperature (K)	823
Coolant inlet temperature (K)	673
Average coolant outlet temperature (K)	753
Average coolant velocity ($m\,s^{-1}$)	1.4

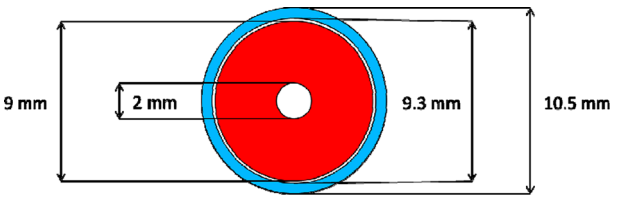

Fig. 2 ALFRED fuel pin cross section

Fuel pin mechanical pattern is taken from ELFR [2]. The bundle is formed with the help of a T91 wrapper enclosing 127 fuel pins arranged in the triangular lattice. In order to comply with 5 MPa pressure of fission gases, the axial extension of plenum and spring has been set

Table 2 ALFRED fuel pin specifications

Parameters	Value
Fuel pellet inner diameter (mm)	2
Fuel pellet outer diameter (mm)	9
Cladding inner diameter (mm)	9.3
Cladding outer diameter (mm)	10.5
Lower plenum length (mm)	550
Active length (mm)	600
Upper plenum length (mm)	120
Pin pitch (mm)	13.86
Pre pressurization (MPa)	0.1
Fill gas	He
Cladding	Ti-15-15
O/M	1.97
Fuel density of theoretical density (%)	95
Pu/(Pu+U) enrichment (inner zone) (wt%)	21.7
Pu/(Pu+U) enrichment (outer zone) (wt%)	27.8
Fuel	MOX

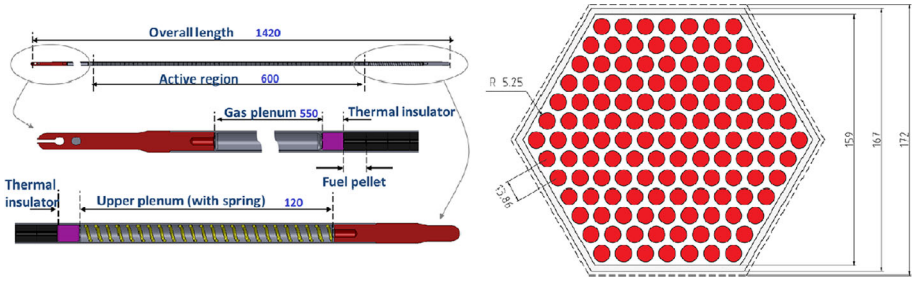

Fig. 3 Alfred fuel pin and FA cross section

for completing the design of fuel pin. The horizontal view of ALFRED fuel pin and assembly is shown in Fig. 3.

The fuel assemblies are arranged in a way to provide a cylindrical core for ALFRED reactor. Sixteen control and safety rods are predicted for reactor safety and control. The design pattern of safety and control rods is derived from CDT-MYRRHY project [16]. The excess reactivity is controlled by two types of control rods, namely control rods (CRs) and safety rods (SRs). While the first one regulates the power and reactivity swing during the life cycle, the second one has safety purposes. CRs are cylindrical shape bundles of 19 pins having B_4C as an absorber material whereas SRs are made of 12 pins with the same material. Figure 4 depicts the SR and CR proposed for the reactor core of ALFRED.

3 Thermal-hydraulic model

OpenFOAM is applied for the thermal-hydraulic analysis of ALFRED fuel assembly. It's an open-source C++ software for computational fluid dynamics (CFD) which solves the

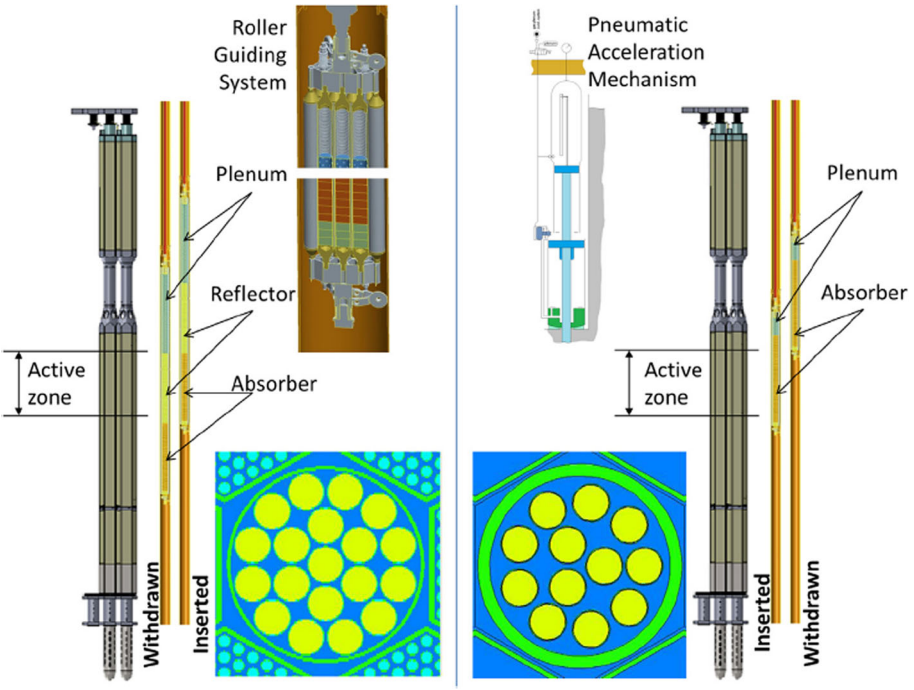

Fig. 4 CR (left) and SR (right) of ALFRED reactor

required equations in finite volume discretization. ChtMultiRegionSimpleFoam solver is a heat conjugate transfer (HCT) solver adopted and used for thermal-hydraulic analysis. The model of fluid flow is based on Reynolds-averaged Navier–Stokes (RANS) equations for mass and momentum conservations. The essential equations related to mass, momentum and energy conservations are as follows:

$$\frac{\partial \rho}{\partial t} + \vec{\nabla}.(\rho \vec{\mathbf{u}}) = 0 \tag{1}$$

$$\rho \frac{\partial (\mathbf{u})}{\partial t} + \rho(\mathbf{u}.\nabla)\mathbf{u} = \nabla.\left(-p\mathbf{I} + (\mu + \mu_T)((\nabla \mathbf{u}) + (\nabla \mathbf{u})^T) - \frac{2}{3}\rho k \mathbf{I}\right) - g\rho \tag{2}$$

$$\rho c_p \frac{\partial T}{\partial t} + \rho c_p \mathbf{u}.\nabla T = \nabla.(\boldsymbol{\lambda} \nabla T) + Q \tag{3}$$

k-ε model is used as a turbulence model [17], where k is the turbulence kinetic energy and ε is the turbulence dissipation rate calculated based on the following equations.

$$\frac{\partial (\rho k)}{\partial t} + \nabla \cdot (\rho \mathbf{u} k) - \nabla \cdot (\rho D_k \nabla k) = G_k - \frac{2}{3}\rho(\nabla \cdot \mathbf{u})k - \rho\varepsilon + S_k \tag{4}$$

$$\frac{\partial (\rho \varepsilon)}{\partial t} + \nabla \cdot (\rho \mathbf{u} \varepsilon) - \nabla \cdot (\rho D_\varepsilon \nabla \varepsilon) = \frac{C_1 G_k \varepsilon}{k} - \left(\frac{2}{3}C_1 + C_{3,\mathrm{RDT}}\right)\rho(\nabla \cdot \mathbf{u})k - C_2 \rho \frac{\varepsilon^2}{k} + S_\varepsilon \tag{5}$$

These two equations in OpenFOAM are different from the original k-ε model. The second term on the right-hand side (r.h.s) incorporates the rapid distortion theory (RDT) contribution,

Table 3 Constant parameters applied in the OpenFOAM solver for $k-\varepsilon$ turbulence model

C_μ	C_1	C_2	$C_{3,RDT}$
0.09	1.44	1.92	−0.33

Table 4 Constants used for the calculation of thermal conductivity of PuO_2 using COMETHE formulation

Constant	Value
A_0	40.05
A_1	129.4
A_2	16020
B_0	0.8
C_h	0.6416E−12

buoyancy contribution is not included, and the coefficient C_3 is not the same as $C_{3,RDT}$ [7]. Table 3 shows the default model coefficients applied in OpenFOAM model.

For isotropic turbulence, the turbulence kinetic energy can be estimated by:

$$k = \frac{3}{2}(U_0 I_T)^2 \tag{6}$$

where I is the intensity and U is a reference velocity. The turbulence dissipation rate is as follows

$$\varepsilon = C_\mu^{\frac{3}{4}} \frac{k^{\frac{3}{2}}}{L_T} \tag{7}$$

where C_μ is a constant equal to 0.009 and L is a reference length scale.

3.1 Thermophysical properties of fuel

3.1.1 Thermal conductivity

Thermal conductivity is dependent on various parameters of UO2 and MOX fuels such as density, oxygen content, composition or deviation from stoichiometry. Thermal conductivity declines by temperature increase up to 2000 K and then augments. Additional use of PuO2 into the fuel matrixes reduces thermal conductivity and so does the deviation of oxygen-to-metal ratio from two [10].

The COMETHE formulation is applied for the calculation of MOX fuel. Taking into account plutonium weight percentage based on the data from Ref. [11], the thermal conductivity is obtained from:

$$K(T) = \frac{A_0}{A_1 + A_2 x + (1 + B_0 q)T} + C_h T^3 \ (\mathrm{W/cm/^\circ C}) \tag{8}$$

where x is the absolute value of the stoichiometry deviation and q is the plutonium content. Table 4 shows the constants used for the calculation of thermal conductivity of PuO_2 using COMETHE formulation. Figure 5 shows the MOX thermal conductivity variation versus temperature using COMETHE formulation.

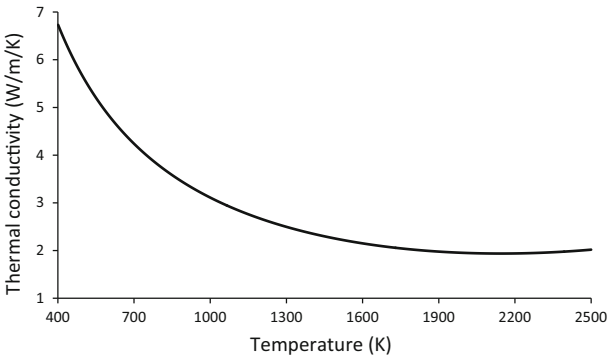

Fig. 5 Thermal conductivity of MOX versus temperature using COMETHE formulation

Table 5 Constants used for heat capacity correlation

Constant	UO_2	PuO_2	Units
C_1	− 78.4303	− 118.2062	J/kg
C_2	193.238	311.7866	J/kg/K
C_3	162.8647	19.629	J/kg/K^2
C_4	− 104.0014	− 0.752	J/kg/K^3
C_5	29.2056	0	J/kg/K^4
C_6	− 1.9507	0	J/kg/K^5
C_7	2.6441	7.0131	J K/kg

3.1.2 Heat capacity

The enthalpy and heat capacity are calculated by a correlation based on the Neumann–Kopp law recommended by Ref. [18]. Although Kopp's law is validated for low Pu content MOX fuel only up to (1573 K), in Ref. [19] it was assumed that this law is still valid at higher temperature to calculate the conductivity data up to 2000°C. In this work, however, the recommended correlation proposed by Ref. [12] is implemented in order to calculate the heat capacity for higher temperatures. The heat capacity can be defined as:

$$C_p = C_2 + \frac{1}{1000}(2C_3T + 3C_4T^2 + 4C_5T^3 + 5C_6T^4 - C_7T^{-2})\ (\mathrm{J\,kg^{-1}\,K^{-1}}) \quad (9)$$

The constants required to calculate heat capacity are depicted in Table 5. And the heat capacity of the MOX is achieved by the following formula:

$$C_p(T, MOX) = (1-q)C_p(T, UO_2) + qC_p(T, PuO_2)\ (\mathrm{J\,kg^{-1}\,K^{-1}}) \quad (10)$$

Figure 6 shows the variation of heat capacity of MOX in terms of temperature variation.

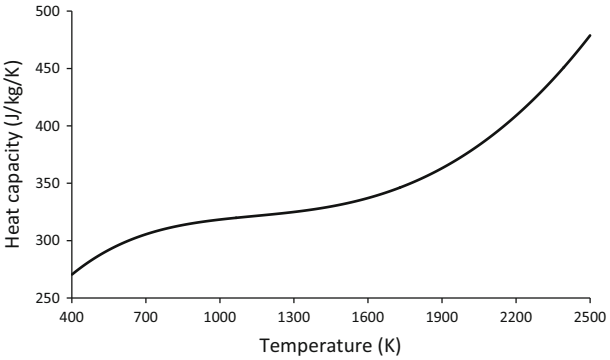

Fig. 6 Heat capacity of MOX versus temperature using Fink's correlation

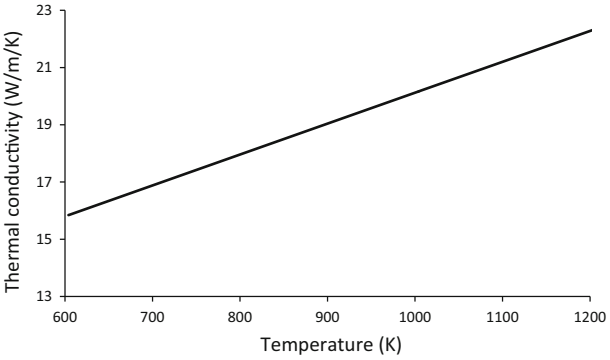

Fig. 7 Thermal conductivity of liquid lead versus temperature

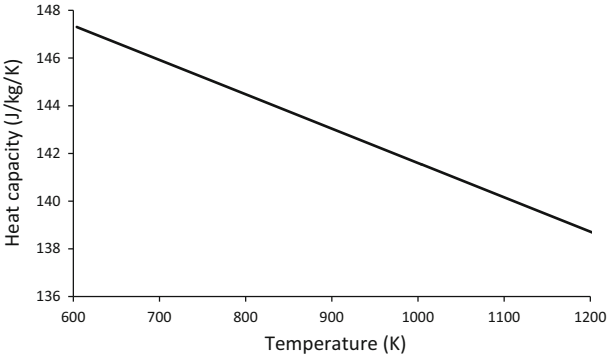

Fig. 8 Lead heat capacity variation versus temperature

3.2 Thermophysical properties of coolant

3.2.1 Thermal conductivity

Thermal conductivity applied in thermal-hydraulic calculation for the coolant is obtained from a correlation as defined in Ref. [13]:

$$K(T) = 9.32 + 0.0108T \ (\mathrm{Wm^{-1}\,K^{-1}}) \tag{11}$$

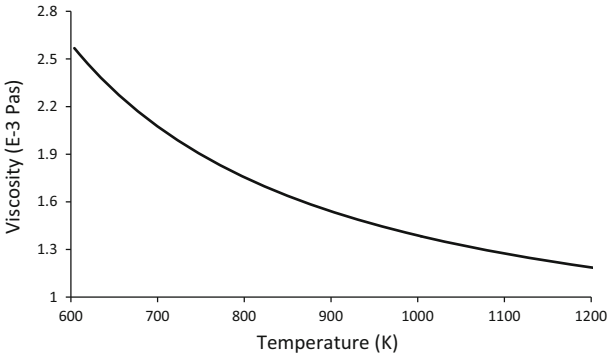

Fig. 9 Variation of viscosity versus temperature for liquid lead

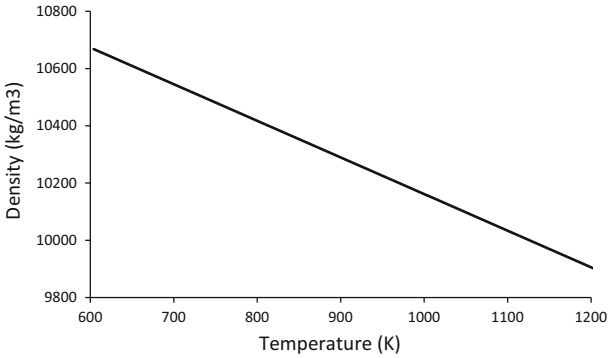

Fig. 10 Density variation versus temperature for liquid lead

Figure 7 depicts the coolant thermal conductivity variation versus temperature.

3.2.2 Heat capacity

The heat capacity can be calculated from the following interpolated function for the liquid lead:

$$C_p = 156 - 0.0144T \ (\mathrm{J\,kg^{-1}\,K^{-1}}) \tag{12}$$

The coolant heat capacity is shown in Fig. 8.

3.2.3 Viscosity

The viscosity as a function of temperature is calculated as follows and is shown in Fig. 9.

$$\eta(T) = 5.43E - 4\mathrm{e}^{\frac{938.5}{T}} \ (\mathrm{Pas}) \tag{13}$$

3.2.4 Density

The density of liquid lead is considered according to the following correlation [14]. Its variation versus temperature is depicted in Fig. 10.

$$\rho(T) = 11441 - 1.2795T \ (\mathrm{kg/m^3}) \tag{14}$$

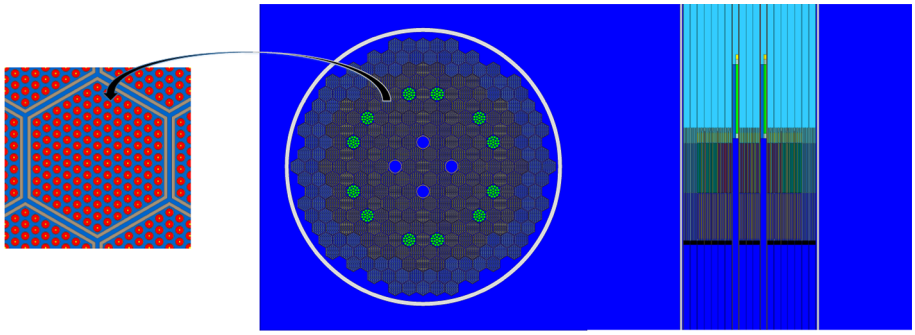

Fig. 11 ALFRED reactor model prepared in Serpent

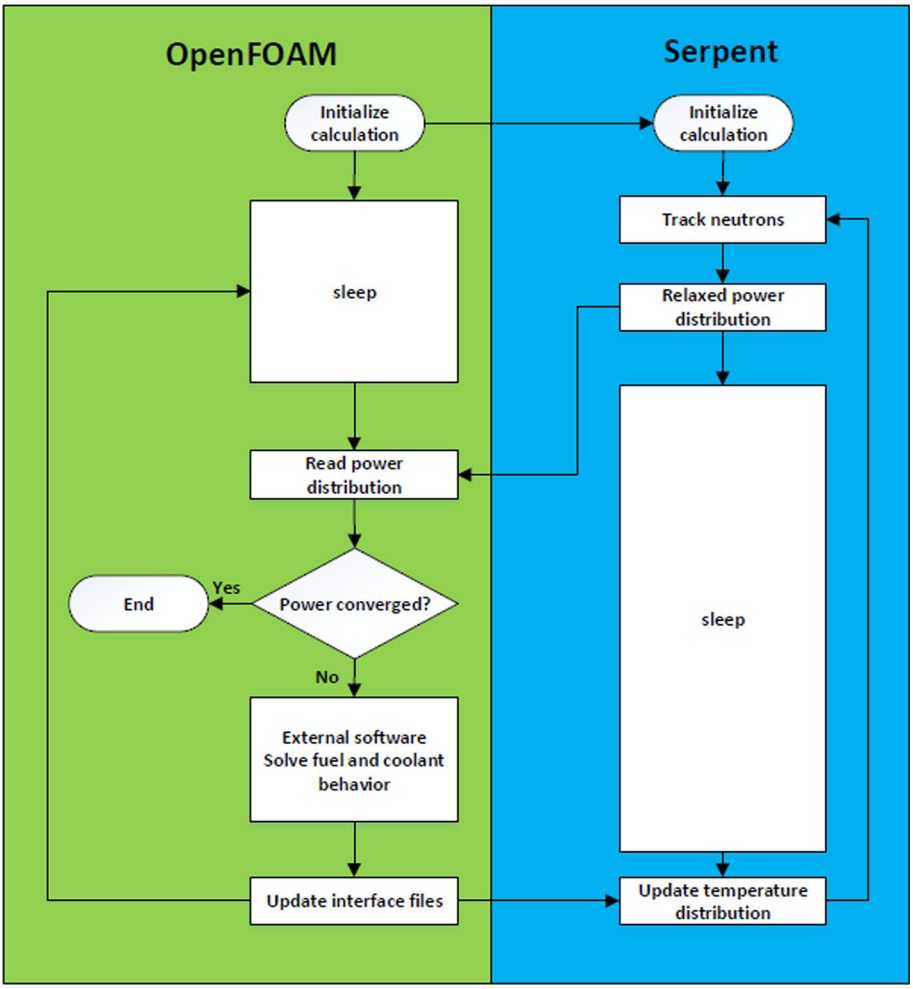

Fig. 12 Mapping procedure for coupled neutronic and thermal-hydraulic calculations

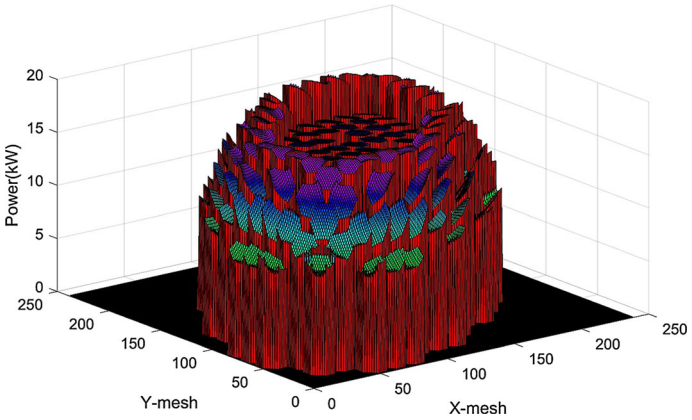

Fig. 13 Fuel pin power distribution of ALFRED reactor initial core

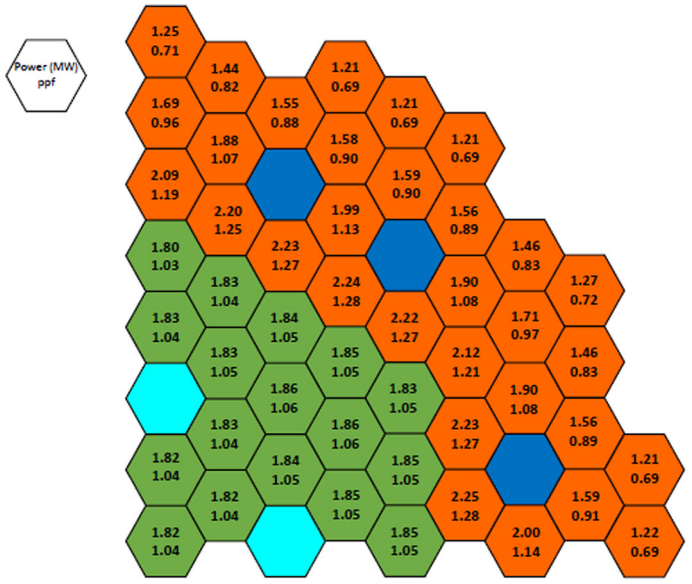

Fig. 14 Power peaking factor of one-fourth of ALFRED reactor initial core

4 Neutronic model

In order to perform the neutronic analysis, a three-dimensional (3D) geometry is adopted for ALFRED reactor core using Serpent, a continuous-energy Monte Carlo reactor physics code for three-dimensional neutronic calculation of nuclear reactors with various applications ranging from homogenized group constant generation to burnup calculations [20]. Target motion sampling (TMS) on-the-fly treatment technique is implemented in Serpent 2. The TMS method accounts for thermal motion explicitly, by making a coordinate transformation in the target-at-rest frame before handling the collision physics instead of averaging the cross sections over the Maxwellian distribution [21]. JEFF 3.1.1 library is used in order to obtain the cross sections for various materials applied in reactor structures. 4.5% of enrichment is

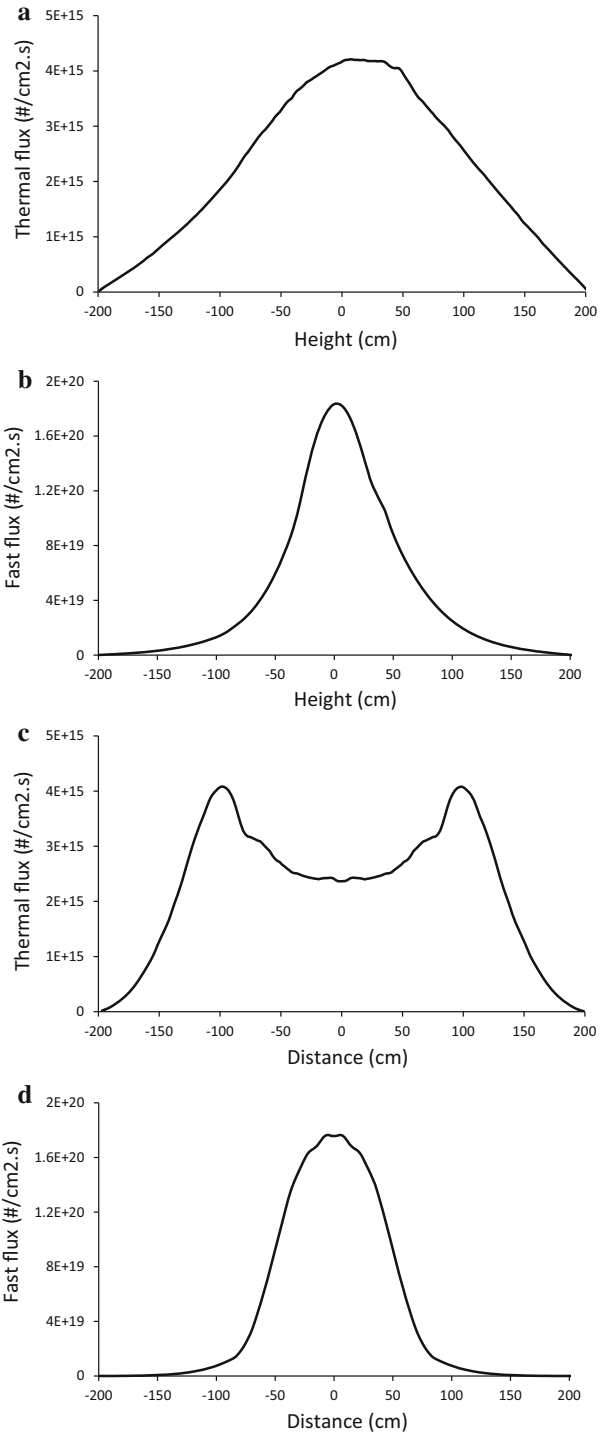

Fig. 15 Core flux distribution of ALFRED reactor: **a** axial thermal flux, **b** axial fast flux, **c** radial thermal flux, **d** radial fast flux

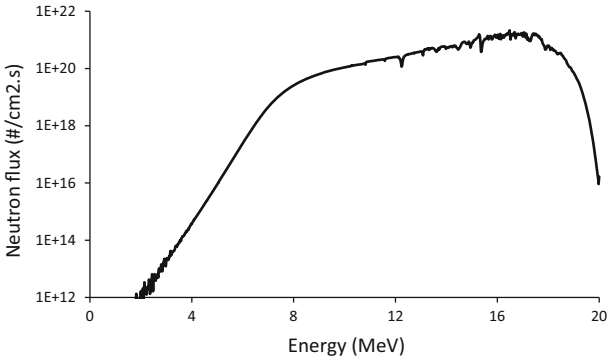

Fig. 16 Neutron spectrum for ALFRED reactor core

considered for ^{235}U. The final configuration satisfying the design goals has been achieved considering 57 fuel assemblies (out of 171) in the inner core zone, with fuel enrichment at 21.7% (Pu $+^{241}$ Am)/(Pu $+^{241}$ Am + U), and in the outer zone 114 fuel assemblies with fuel enriched at 27.8% [2]. The fuel pin, fuel assembly and other components of the core are modeled as mentioned by the reference core. Figure 11 shows the ALFRED reactor model prepared in Serpent.

In this paper, several neutronic parameters such as thermal and fast flux distribution, power density distribution, power peaking factor, neutron spectrum, and control and safety rods worth are calculated. All of the calculations performed in this paper are related to the reactor initial core.

5 Relaxation and convergence

A natural characteristic of stochastic procedure is that converged results are challenging since the same input does not always induce the same output. In fact, the same temperature and density distributions do not always guarantee the same outcome. Thus, a procedure should be specified in order to evaluate the convergence. Since in multi-physics modeling the power is calculated in each iteration and inserted in OpenFOAM, a relaxation scheme based on stochastic approximation is adopted according to the following formula for its convergence [22]:

$$P_{\text{rel}}^{(n+1)} = P_{\text{rel}}^{(n)} - \frac{s_{n+1}}{\sum_{i=1}^{n+1} s_i}\alpha(P_{\text{rel}}^{(n)} - P^{(n+1)}) \tag{15}$$

where $P_{\text{rel}}^{(n+1)}$ and $P_{\text{rel}}^{(n)}$ are the relaxed power distributions on iterations $n + 1$ and n respectively. $P^{(n+1)}$ is the iteration wise power distribution on iteration $n + 1$, s_i is the number of simulated neutrons on iteration i and α is an additional under-relaxation factor. In order to check the convergence of the temperature, a relative power variation function is implemented as follows.

$$P_r^{n+1} = \sum_{h'=1}^{N_f} \left| \frac{P_{h',n+1} - P_{h',n}}{P_{h',n+1}} \right| \tag{16}$$

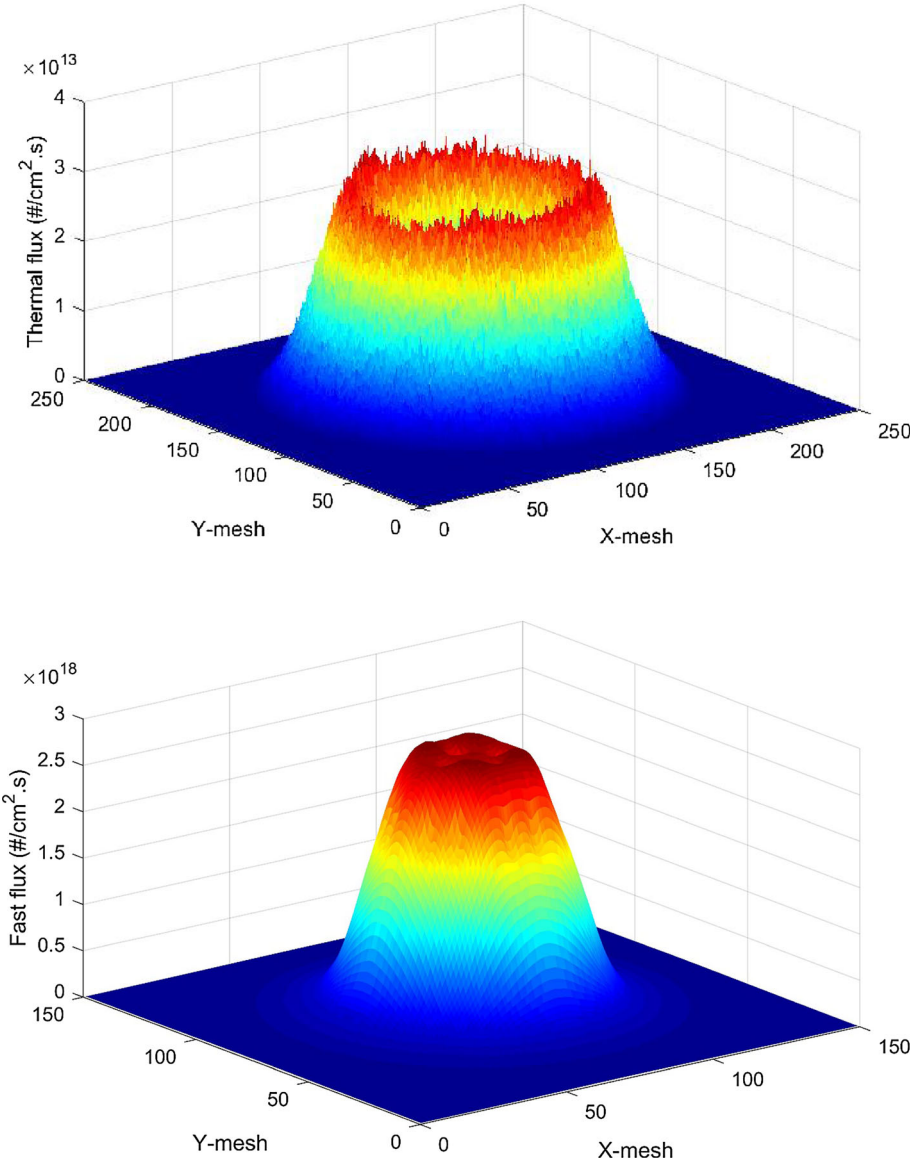

Fig. 17 Thermal and fast flux distribution of ALFRED reactor core

where $P_{h',n+1}$ and $P_{h',n}$ are the power distributions of h'th fuel element at the iteration of $n+1$ and n respectively. Also N_f is the number of fuel elements in the thermal-hydraulic model.

Table 6 Neutronic parameters calculated for ALFRED reactor initial core

Parameter	Unit	MCNPX [2]	ERANOS [2]	SERPENT
Max power in fuel assembly	MW	2.21	2.42	2.25
Total worth of 12 CRs	pcm	−8500	−9100	−8511
Total worth of 4 SRs	pcm	−3300	−3700	−2957
ppf_{max}	–	–	–	1.28
Effective delay neutron fraction	pcm	–	336	336

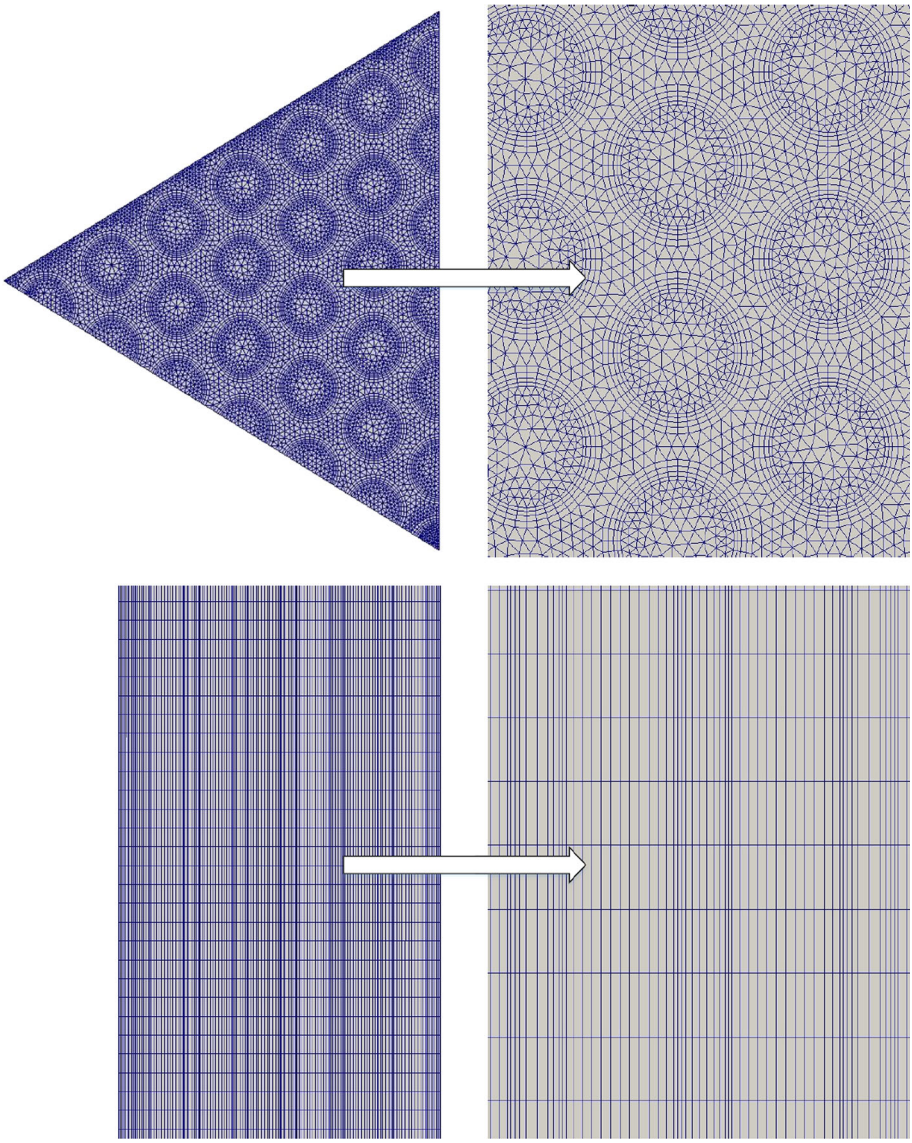

Fig. 18 Unstructured mesh prepared for the thermal-hydraulic analysis of the fuel assembly

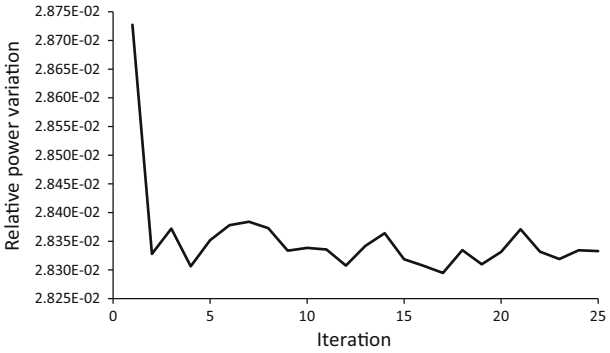

Fig. 19 Relative power variation versus iteration for the Serpent–OpenFOAM coupling procedure

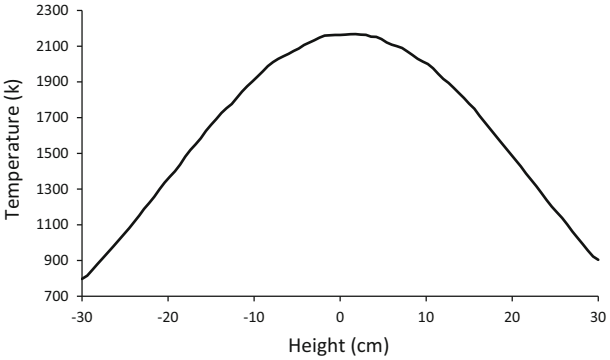

Fig. 20 Temperature distribution in central fuel pin of the most powerful fuel assembly of ALFRED

6 Coupled neutronic thermal-hydraulic procedure

A program was written in MATLAB in order to map the multi-physics modeling procedure. According to Fig. 12, the program starts by initializing the parameters for both OpenFOAM and Serpent. This procedure is pursued by considering one million neutrons in one thousand cycles. After the neutronic calculation is carried out, the power is relaxed as previously discussed. While the serpent goes to the sleep state, the OpenFOAM solver commences its job by running the heat conjugate transfer (HCT) solver for performing computational fluid dynamics (CFD) calculations. However, in terms of convergence, firstly the convergence of the power needs to be evaluated. In case the power is not converged, the program keeps running. Otherwise, the program finishes and the final results are obtained. When the power density distribution is calculated and inserted in OpenFOAM by serpent interfaces, the solver initializes its CFD calculations using k-ε turbulence model. Up to now, the first iteration is finished. For the upcoming iterations, the interfaces for the power and temperature exchanges need to be updated. Also, the temperature distribution for the next neutronic calculation should be updated. This procedure is continued until a convergence is accomplished.

7 Neutronic calculation analysis

ALFRED reactor was modeled in Serpent, and its neutronic parameters were obtained. In this simulation, JEFF 3.1.1 was applied as nuclear data library. Reactor operative power

Table 7 The maximum temperature of the hottest fuel pin in ALFRED

Method	Fluent CFD & ANTEO-LFR [2]	Serpent–OpenFOAM coupling
Value (k)	2204	2167

was deemed 300 MWth for steady-state neutronic analysis. While Fig. 13 shows the power distribution of fuel pins, in Fig. 14 the power peaking factor (ppf) of fuel assembles inside one-forth of the initial core is shown. The maximum ppf is 1.28, which is related to the fuel assembly with the highest power of 2.25 MW in the core. This power value is also taken into account for thermal-hydraulic analysis. Unfortunately, since ALFRED reactor is still under design and development, not all of the data are validated to be benchmarked. An investigation was carried out in order to obtain the flux distribution inside the reactor. Thermal and fast flux distributions were achieved radially and axially. Figure 15 depicts the axial and radial flux inside ALFRED reactor core. There is a small diversion form of symmetric shape of flux distribution, and it's probably due to the inequality of the upper and lower plenum size in the fuel rods. Moreover, a 3D distribution of thermal and fast flux in core is shown in Fig. 16. Neutron spectrum for ALFRED reactor core is also shown in Fig. 17. The worth of control rods and safety rods was computed as well. Table 6 shows the neutronic parameters calculated by serpent for ALFRED reactor. These parameters are also evaluated with the calculation performed by MCNPX and ERANOS [23] in Ref. [2]. There is a good agreement between the computed data and the parameters mentioned in the reference.

8 Fuel assembly thermal-hydraulic analysis

With an application of OpenFOAM, thermal-hydraulic analysis of the assembly with the maximum power was carried out. A fuel assembly with the power of 2.25 MW was implemented in Serpent in order to obtain the power distribution. Its x and y coordinates were specified as reflective boundaries.

The thermal-hydraulic analysis was carried out by the power density distribution linked from Serpent–OpenFOAM interface. ChtMultiRegionSimpleFoam was applied as a solver for heat conjugate transfer (HCT) considering Reynolds-averaged Navier–Stokes (RANS) equations to perform CFD calculations. k-ε turbulence model was adopted in thermal-hydraulic analysis. However, in terms of simplicity, one-sixth of the fuel assembly was modeled in OpenFOAM. A thermal resistance was considered for cladding coating with 40 μm thickness and thermal conductivity of 15 $W\,m^{-1}\,K^{-1}$ [24]. A mesh sensitivity analysis was carried out in order to find a proper mesh for thermal-hydraulic analysis. The unstructured mesh implemented for thermal-hydraulic calculation in OpenFOAM is depicted in Fig. 18.

Temperature and velocity distributions were obtained by coupling Serpent and OpenFOAM taking into account that from the place where two planes of the fuel assembly were cut into one-sixth, it was taken as symmetry for all the calculated parameters. Relative power variation is shown in Fig. 19. The result shows that the convergence is limited to 0.005% of difference for the final result due to the natural effect of the application of Monte Carlo method for the calculation of power distribution in multi-physics modeling.

Temperature distribution in the central fuel pin of the fuel assembly in axial direction is shown in Fig. 20. It is seen that the temperature of the central fuel pin is 2167 K which does

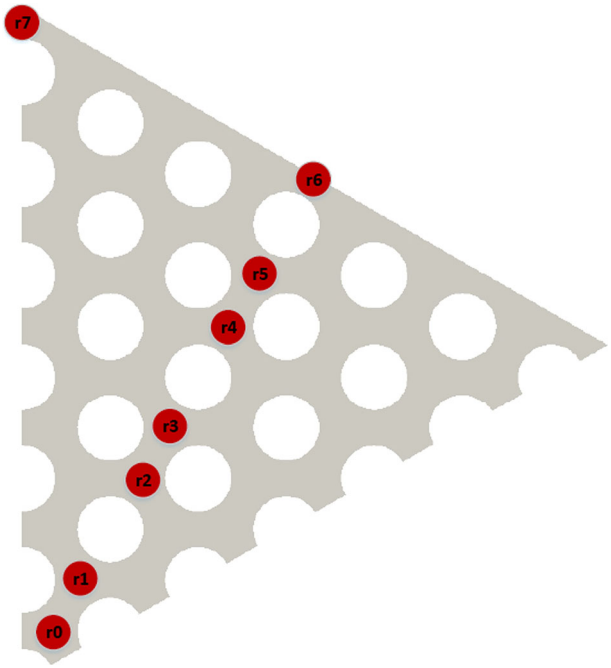

Fig. 21 Specified points for the calculation of temperature and velocity distribution in one-sixth of the fuel assembly

not exceed the limited temperature (2273 K) specified for the fuel pin. Other investigation was to examine the maximum temperature in the hottest fuel pin. Table 7 shows the maximum temperature obtained for the hottest fuel pin. It is observed that there is a good agreement between the calculated result and the value which was previously defined. The results have 1.68% of difference.

Furthermore, an investigation was carried out in order to examine the axial variation of temperature and velocity distributions in different parts of the fluid in the fuel assembly. Different locations in the fuel assembly were marked. Figure 21 shows the points in different sub-channels for the calculation of temperature and velocity distributions.

Figure 22 shows the temperature and velocity distribution points from r to r_6 related to six sub-channels inside the fuel assembly. The results show that the fluid in all of the sub-channels has identical distribution for temperature and velocity except the last one, which has the highest temperature in the center of fuel assembly and lowest one on the top. Also, the velocity in the last sub-channel is always less than the other sub-channels although it is increasing at first.

The temperature and velocity distributions are shown in Fig. 23.

In the outer part of the fuel assembly's corner, the velocity was decreased drastically. The temperature and velocity in r7 which are related to the upper left corner of fuel assembly are shown in Fig. 24. Although the velocity was decreased in this sub-channel, the temperature was below the average coolant temperature (753 K) in the axial direction. Therefore, these results show that the velocity and temperature for the coolant and fuel in this multi-physics modeling are well maintained for ALFRED initial reactor core.

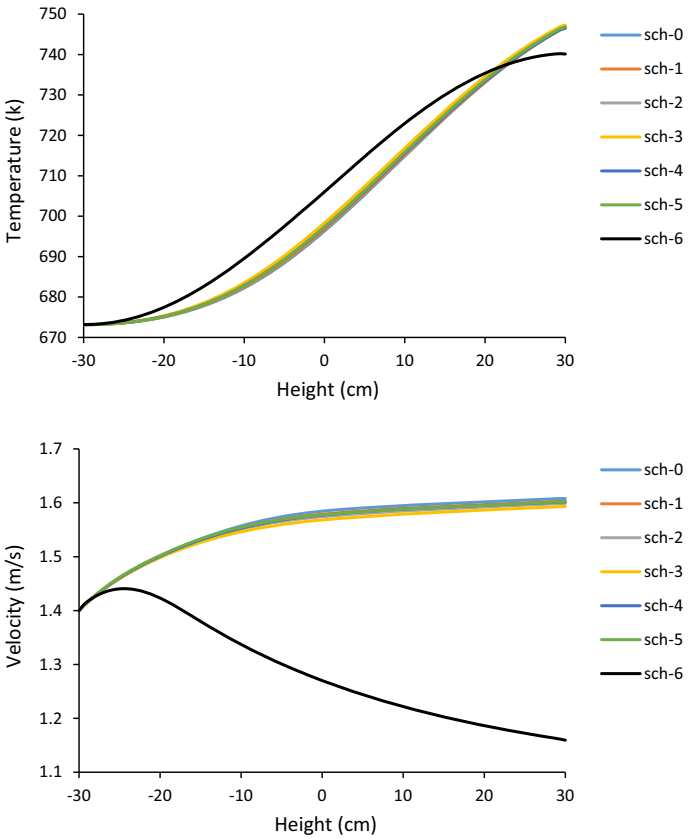

Fig. 22 Temperature and velocity distribution in the fuel assembly with the maximum power

9 Conclusions

The objective of this paper was to introduce a multi-physics model for neutronic and thermal-hydraulic analysis of Advanced Lead Fast Reactor Demonstrator (ALFRED). Neutronic calculation for the initial core was performed in Serpent Monte Carlo calculation code using JEFF 3.1.1 library for neutron cross sections. A three-dimensional (3D) geometry of ALFRED reactor core was prepared for obtaining the neutronic parameters. The power distribution for fuel assemblies was calculated, and the fuel assembly with the maximum power was pinpointed and used in thermal-hydraulic analysis. For simplicity, a symmetric 3D model of one-six of the fuel assembly was prepared in OpenFOAM, a software written in C++ language to solve Reynolds-averaged Navier–Stokes (RANS) equations for computational fluid dynamics (CFD) calculations. k-ε turbulence model was adopted for thermal-hydraulic analysis. A solver with the capability of heat conjugate transfer (HCT) calculation was implemented to calculate the temperature and velocity distributions inside the fuel assembly. An approach was carried out in order to investigate the convergence of the coupling method. The coupling procedure shows that the fuel and coolant temperatures do not exceed the predefined values and therefore perform well for the initial core. The results show that the multi-physics modeling is a promising procedure to predict the phenomena in LFR reactor,

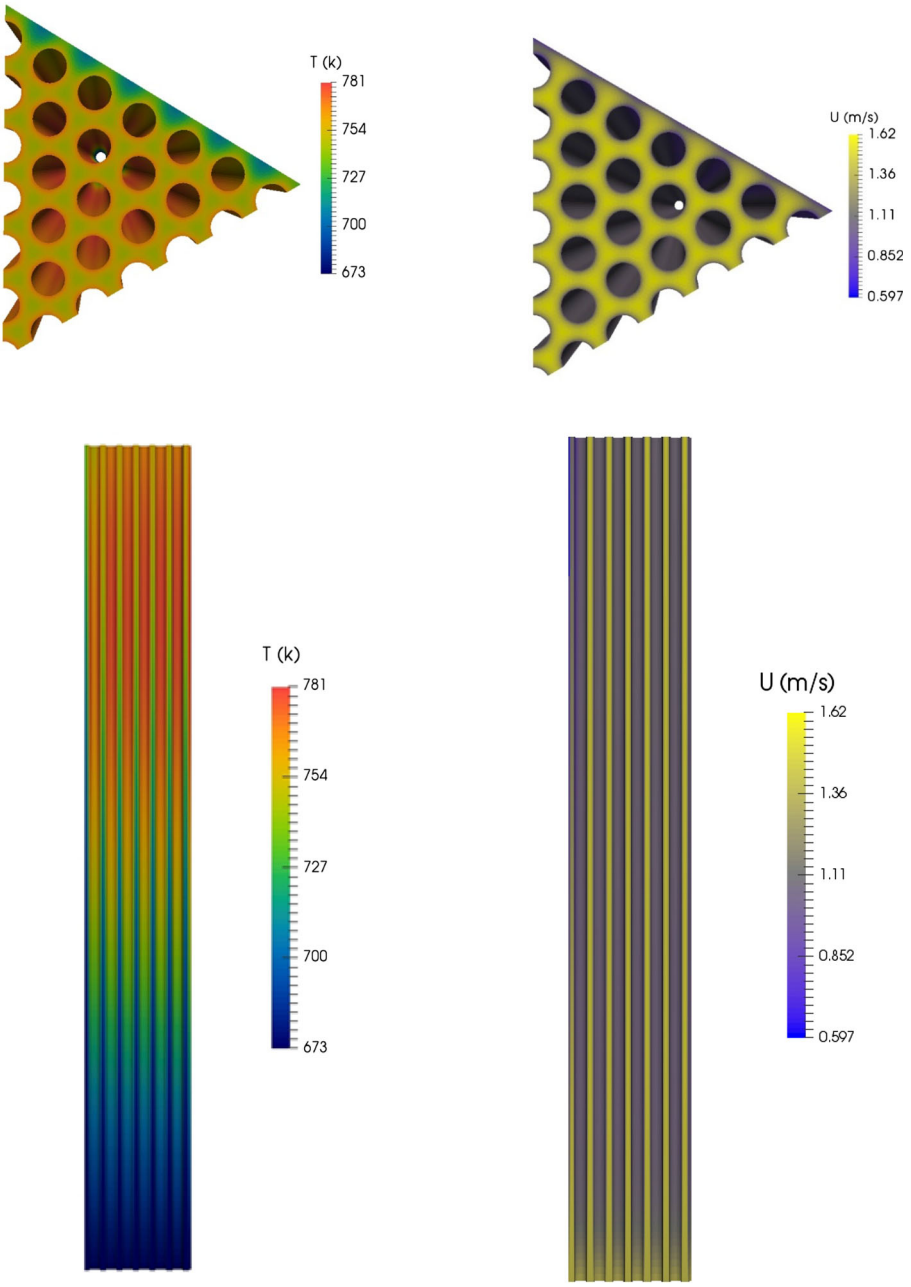

Fig. 23 Temperature and velocity distributions in the fuel assembly with the maximum power

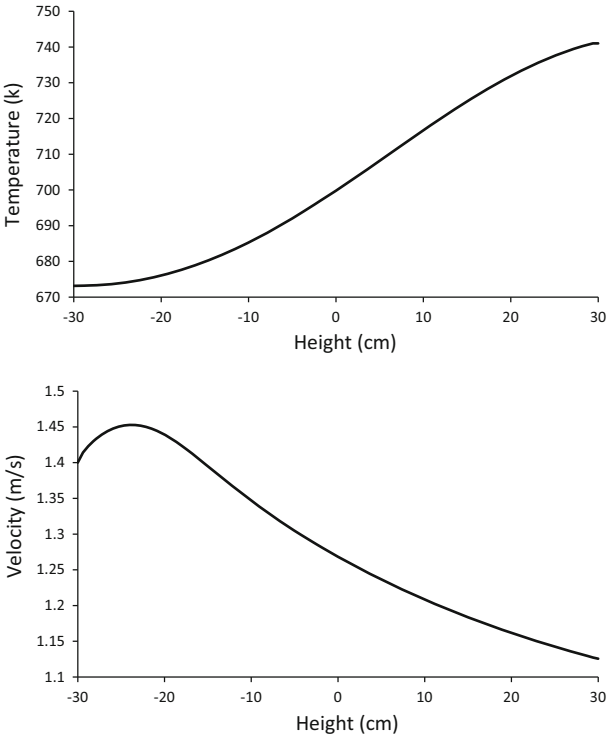

Fig. 24 Temperature and velocity distributions of the upper corner of the fuel assembly with the maximum power

which can not only be applied for neutronic and thermal-hydraulic analysis, but also can be considered for other problems such as solidification and corrosion. A new work is also under implementation for the sensitivity analysis of the turbulence model applied in multi-physics coupling of ALFRED.

Acknowledgements The authors wish to express their thanks to the management and staff of CeSNEF-Nuclear Engineering Division, Department of Energy, Politectico di Milano, Milano, Italy, for their support and contribution.

References

1. A. Alemberti, D. De Bruyn, G. Grasso, L. Mansani, D. Mattioli, F. Roelofs, *Presented at the FR13-IAEA International Conference on Fast Reactors and Related Fuel Cycles: Safe Technologies and Sustainable Scenarios, Paris* (2013) (unpublished)
2. G. Grasso, C. Petrovich, D. Mattioli, C. Artioli, P. Sciora, D. Gugiu, G. Bandini, E. Bubelis, K. Mikityuk, Nuclear Eng. Des. **278**, 287 (2014)
3. N. Cerullo, G. Lomonaco IV, *Nuclear Fuel Cycle Science and Engineering*, ed. by I. Crossland (Woodhead Publishing: Cambridge, UK, 2012), p. 333
4. C.F. Smith, L. Cinotti, *Handbook of Generation IV Nuclear Reactors* (Elsevier, Amsterdam, 2016), p. 119
5. D. Chersola, G. Lomonaco, R. Marotta, G. Mazzini, Nuclear Eng. Des. **273**, 542 (2014)

6. D. Chersola, G. Lomonaco, G. Mazzini, *Presented at the 2014 22nd International Conference on Nuclear Engineering* (2014) (unpublished)
7. OpenFOAM, in www.openfoam.org (2017)
8. G. Lomonaco, W. Borreani, M. Bruzzone, D. Chersola, G. Firpo, M. Osipenko, M. Palmero, F. Panza, M. Ripani, P. Saracco, Therm. Sci. Eng. Prog. **6**, 447 (2018)
9. J.F. Fernández, Universitat Politècnica de Catalunya (UPC) (2012)
10. J.J. Carbajo, G.L. Yoder, S.G. Popov, V.K. Ivanov, J. Nuclear Mater. **299**(3), 181 (2001)
11. D. Baron, *Presented at the Proceedings of Seminar on Thermal Performance of High Burnup LWR Fuel* (1998) (unpublished)
12. J. Fink, J. Nuclear Mater. **279**(1), 1 (2000)
13. P. Kirillov, *Institute for heat and mass transfer in nuclear power plants* (Obninsk, 2006)
14. V. Sobolev, P. Schuurmans, G. Benamati, J. Nuclear Mater. **376**(3), 358 (2008)
15. G. Grasso, C. Petrovich, K. Mikityuk, D. Mattioli, F. Manni, D. Gugiu, *Presented at the Proceedings of the IAEA International Conference on Fast Reactors and Related Fuel Cycles: Safe Technologies and Sustainable Scenarios* (2013) (unpublished)
16. D. Lamberts, *presented at the SCK · CEN/PSD, LEADER Project Meeting, Bologna, 25th October* (2011) (unpublished)
17. B.E. Launder, D.B. Spalding, Comput. Methods Appl. Mech. Eng. **3**(2), 269 (1974)
18. Y. Philipponneau, J. Nuclear Mater. **188**, 194 (1992)
19. C. Duriez, J.-P. Alessandri, T. Gervais, Y. Philipponneau, J. Nuclear Mater. **277**(2), 143 (2000)
20. J. Leppänen, VTT Technical Research Centre of Finland **4**, (2013)
21. T. Viitanen, J. Leppänen, Nuclear Sci. Eng. **177**(1), 77 (2014)
22. J. Dufek, W. Gudowski, Nuclear Sci. Eng. **152**(3), 274 (2006)
23. G. Rimpault, D. Plisson, J. Tommasi, R. Jacqmin, J. Rieunier, D. Verrier, D. Biron, *presented at the Proceedings of International Conference on PHYSOR* (2002) (unpublished)
24. A. Weisenburger, A. Heinzel, G. Müller, H. Muscher, A. Rousanov, J. Nuclear Mater. **376**(3), 274 (2008)